A study on the performances of the run sum $\bar{X}$ chart under the gamma process

Kai Le Goh[1], *Wei Lin* Teoh[1*], *Zhi Lin* Chong[2], *Kai Lin* Ong[1], and *Laila* El-Ghandour[3]

[1]School of Mathematical and Computer Sciences, Heriot-Watt University Malaysia, 62200 Putrajaya, Malaysia
[2]Department of Electronic Engineering, Faculty of Engineering and Green Technology, Universiti Tunku Abdul Rahman, 31900 Perak, Malaysia
[3]School of Mathematical and Computer Sciences, Heriot-Watt University, Edinburgh, Currie EH14 4AP, United Kingdom

Abstract. The run sum (RS) $\bar{X}$ chart is known as a simple and powerful tool for monitoring the mean of a process. Most developments of the RS $\bar{X}$ chart assume that the underlying process comes from a normal distribution. However, in practice, many processes tend to follow a non-normal distribution. These non-normal processes affect the performances of control charts under the design of normal distribution. In this paper, we present a detailed analysis on the performances of the RS $\bar{X}$ chart when the underlying data come from a gamma distribution. By using Monte Carlo simulation approach, the run-length properties, namely the average run length and the standard deviation of the run length will be computed. Particularly, the 4 and 7 regions RS $\bar{X}$ charts under both distributions are considered. When the charts' parameters specifically designed for the normal distribution are used to monitor the data from a gamma distribution, simulated results show that RS $\bar{X}$ charts' performances are significantly deteriorated. The RS $\bar{X}$ chart has higher false alarm rates when the underlying distribution is gamma.

1 Introduction

Statistical process control (SPC) stands out as a potent and magnificent approach that adopts statistical methodologies to meticulously control the stability of manufacturing and service processes. Applying SPC guarantees the production of high-quality products and services, as well as improving the efficiency of processes. Among the various tools in SPC, the control charting procedure holds a prominent position and is commonly favoured, being increasingly used by practitioners and quality engineers. This is due to the control chart's simplicity and effectiveness in monitoring the process stability over time. For monitoring large process mean shifts, the traditional Shewhart $\bar{X}$ chart is powerful, as originally proposed by Shewhart [1] in 1931. To enhance the sensitivity of detecting small and moderate process mean shifts for the Shewhart $\bar{X}$ chart, Roberts [2] introduced the run sum (RS) scheme as an alternative solution. Subsequently, Reynolds [3] expanded the concept of the RS control chart by introducing and assigning scores to individual regions, thereby establishing the RS $\bar{X}$ chart.

*Corresponding author : wei_lin.teoh@hw.ac.uk

Generally, the RS $\bar{X}$ control chart is designed by dividing the $\bar{X}$ chart into several scoring zones or regions around the centre line (CL) and then computing the cumulative RS of the scores. Jaehn [4] proposed a special variant of the RS $\bar{X}$ chart, known as the zone control chart. Davis, Jin, and Guo [5] further studied Jaehn's research [4], introducing a new zone control chart with a fast initial response (FIR) feature. They showed that incorporating common runs rules into the FIR zone control chart enhances its performance compared to the Shewhart $\bar{X}$ chart. Champ and Rigdon [6] formulated the average run length (ARL)-based RS $\bar{X}$ chart by means of the Markov chain technique. They revealed that the RS $\bar{X}$ chart with surpasses the Shewhart $\bar{X}$ chart supplemented with runs rules. In addition, their study demonstrated that by adding a greater number of regions and scores, the detection speed of the RS $\bar{X}$ chart in detecting process mean shifts is superior to the exponentially weighted moving average and cumulative sum $\bar{X}$ charts [6]. A flexible zone individuals control chart was designed and a study between RS and R charts was conducted by Parkhideh and Parkhideh [7] and Aguirre-Torres and Reyes-López [8], respectively. Davis and Krehbiel [9] claimed that the zone control chart with run rules has better performance than the Shewhart $\bar{X}$ chart in the presence of linear trend in process mean over time. Acosta-Mejia and Pignatiello [10] discovered that the FIR RS R control chart is effective in monitoring the variations of process dispersion. Moreover, Sitt, *et al*. [11] proposed the RS t chart and demonstrated its superior effectiveness compared to the RS $\bar{X}$ chart in detecting process variance. Acosta-Mejia and Rincon [12] developed a one-parameter continuous RS chart with the FIR feature. Furthermore, Saha, *et al.* [13] estimated the process parameters to design the RS $\bar{X}$ control chart. Teoh, *et al.* [14] and Lim, *et al.* [15] implemented the univariate and multivariate RS charts, respectively, for monitoring the coefficients of variations (CV). These charts wider the control chart applications in various manufacturing and non-manufacturing scenarios. To further substantiate the effectiveness of the RS control chart, some researchers recently implemented the variable sample interval, variable parameters, and variable sample size and sampling interval schemes for detecting changes in the CV [16-17].

According to the most recent literature, the RS $\bar{X}$ chart is built upon the assumption that the underlying process is characterized by a normal distribution. However, this normality assumption may not hold in real-world industrial scenarios and many processes can exhibit non-normal distributions, particularly the gamma distribution. Some examples include the time to failure of an electronic component in an airborne radar system [18], lifespan of a semiconductor or medical laser [19], lifetime in accelerated life test samples [20], time of detecting the urinary tract infection [21], etc. For this skewed distribution, the control chart designed under the assumption of normality has a high false alarm rate in its Phase II process monitoring [19, 22]. This issue arises due to the dissimilarity in variability patterns between skewed and normal distributions. The negative implications include a reduction of control chart utilizations for process monitoring by practitioners, as well as an increase in extensive time and expensive cost for unnecessary corrective actions due to high false alarm rates.

To date, there has been no exploration regarding the RS $\bar{X}$ chart under the gamma distribution in the existing literature. As a result, this paper conducts a thorough analysis on the performances of the RS $\bar{X}$ chart under the gamma distribution. The layout of this paper is organized in the following order. Section 2 reviews the design of the RS $\bar{X}$ chart under the normal distribution and its run-length properties. Section 3 presents the statistical properties of the gamma distribution. Also, in the same section, we investigate the performances of the RS $\bar{X}$ chart under both the normal and gamma distributions. Last, Section 4 summarizes some key findings and provides future research directions.

2 The RS $\bar{X}$ chart

Suppose that $X_{i,j}$ is the i^{th} sample (for $i = 1, 2, \ldots$) at the j^{th} observation (for $j = 1, 2, \ldots, n$) of a Phase II process, with n representing the sample size. We consider that the observations follow an independent and identically distributed normal distribution, with an in-control mean μ_0 and in-control variance σ_0^2, i.e., $X_{i,j} \sim N(\mu_0, \sigma_0^2)$.

The design of the RS $\bar{X}$ chart involves partitioning the interval between the upper control limit (UCL) and lower control limit (LCL) of the $\bar{X}$ chart into k regions, positioned both above and below the CL, respectively. By referring to Fig. 1., ($\text{CL} < \text{UCL}_1 < \text{UCL}_2 < \cdots < \text{UCL}_k$) and ($\text{LCL}_k < \cdots < \text{LCL}_2 < \text{LCL}_1 < \text{CL}$) represent the UCL and LCL, respectively, above and below the CL. Note that the regions positioned above and below the CL are symmetrical to each other. The assignment of positive ($0 \le S_1 \le S_2 \le \cdots \le S_k$) and negative ($-S_k \le \cdots \le -S_2 \le -S_1 \le 0$) integer scores is designated for each region above and below the CL, respectively. The (R_{+1}, R_{+2}, …, R_{+k}) and (p_{+1}, p_{+2}, …, p_{+k}) are the regions and probabilities above the CL, respectively; while (R_{-1}, R_{-2}, …, R_{-k}) and (p_{-1}, p_{-2}, …, p_{-k}), are referred to the regions and probabilities below the CL, respectively.

In general, the cumulative sums at the i^{th} sample of the RS $\bar{X}$ chart with k regions are as follows:

$$U_i = \begin{cases} U_{i-1} + S_i, \text{if } \bar{X}_i \ge \text{CL} \\ 0 \quad\quad , \text{if } \bar{X}_i < \text{CL} \end{cases} \tag{1}$$

and

$$L_i = \begin{cases} L_{i-1} - S_i, \text{if } \bar{X}_i \le \text{CL} \\ 0 \quad\quad , \text{if } \bar{X}_i > \text{CL} \end{cases}. \tag{2}$$

Here, U_i and L_i represent the upper and lower cumulative sums, respectively. Note that we usually assume $U_0 = L_0 = 0$. The LCL_t, CL and UCL_t are computed as

$$\text{LCL}_t = \mu_0 - K\left(\frac{3t}{k-1}\right)\frac{\sigma_0}{\sqrt{n}}, \tag{3}$$

$$\text{CL} = \mu_0, \tag{4}$$

and

$$\text{UCL}_t = \mu_0 + K\left(\frac{3t}{k-1}\right)\frac{\sigma_0}{\sqrt{n}}, \tag{5}$$

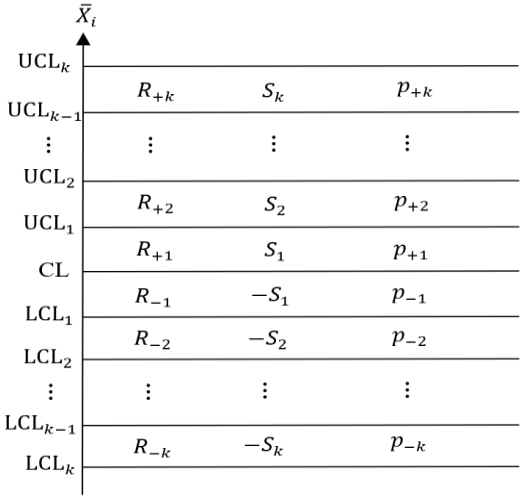

Fig. 1. k regions RS $\bar{X}$ chart (each above and below the CL) with their corresponding control limits, regions, scores, and probabilities.

respectively, for $t = 1, 2, ..., k$. In Equations (3) and (5), the constant parameter K is the control limit coefficient, which needs to be determined to obtain a specified in-control ARL.

Based on Champ and Rigdon [6], the operating procedures of the RS $\bar{X}$ chart with k regions are outlined in the following manner:

1. Select k, the number of regions and compute the control limits LCL_t, CL and UCL_t for $t = 1, 2, ..., k$, using Equations (3) – (5) with their corresponding scores $\pm S_i$.
2. Collect a sample, with a sample size of n and calculate the sample mean $\bar{X}_i = \sum_{i=1}^{n} X_i/n$.
3. Initialize the cumulative scores to 0, i.e., $U_0 = 0$ and $L_0 = 0$.
4. Cumulate the score corresponding to the region where the sample mean $\bar{X}_i$ is located.
5. If $\bar{X}_i$ ($>$ CL) falls in R_t, then compute U_i with Equation (1) and let $L_i = 0$. Conversely, if $\bar{X}_i$ ($<$ CL) falls in R_{-t}, then L_i is computed with Equation (2) and set $U_i = 0$.
6. If $U_i \geq S_k$ or $L_i \leq -S_k$, proceed to Step 7. Otherwise, go back to Step 2.
7. An out-of-control signal is issued, and necessary adjustments are required to bring it back to an in-control state.

The probabilities $p_{+t} = \Pr(\bar{X}_i \in R_{+t})$ and $p_{-t} = \Pr(\bar{X}_i \in R_{-t})$ displayed in Fig. 1. for $t = 1, 2, ..., k$ can be calculated as follows:

$$p_{+t} = \Phi\left[K\left(\frac{3t}{k-1}\right) - \delta\sqrt{n}\right] - \Phi\left[K\left(\frac{3(t-1)}{k-1}\right) - \delta\sqrt{n}\right] \tag{6}$$

and

$$p_{-t} = \Phi\left[-K\left(\frac{3(t-1)}{k-1}\right) - \delta\sqrt{n}\right] - \Phi\left[-K\left(\frac{3t}{k-1}\right) - \delta\sqrt{n}\right], \tag{7}$$

where the function $\Phi(\cdot)$ denotes the cumulative distribution function for the standard normal distribution. For our context, the magnitude of the standardized mean shift is denoted by δ. When $\delta = 0$, the process is deemed statistically in-control; conversely, when $\delta \neq 0$, it is considered statistically out-of-control.

The RS $\bar{X}$ chart is modelled as a discrete-time Markov chain with $v + 1$ states, consisting of transient states 1, 2, ..., v and an absorbing state $v + 1$. Note that v represents the number of possible distinct values associated with the ordered pairs (U_i, L_i) assuming that the underlying process is in an in-control state. The structure of the transition-probability matrix $\mathbf{P}$ for the RS $\bar{X}$ chart is expressed as

$$\mathbf{P} = \begin{pmatrix} \mathbf{Q} & \mathbf{s} \\ \mathbf{0}^T & 1 \end{pmatrix}. \tag{8}$$

Here, $\mathbf{Q}$ represents the $(v \times v)$ transient-probability matrix, $\mathbf{0} = (0, 0, ..., 0)^T$ and $\mathbf{s}$ is the $(v \times 1)$ vector that fulfills $\mathbf{s} = \mathbf{1} - \mathbf{Q1}$ (i.e., the row probabilities must add up to 1) with $\mathbf{1} = (1, 1, ..., 1)^T$. The generic elements and dimensions of the matrix $\mathbf{Q}$ for the RS $\bar{X}$ chart with k regions vary depending on the scores. Generally, the matrix $\mathbf{Q}$ does not have a specified form. The detailed construction of matrix $\mathbf{Q}$ can be referred to the works by Teoh *et al.* [14].

The ARL and standard deviation of the run length (SDRL) for the RS $\bar{X}$ chart by using the Markov chain method are obtained as

$$\mathrm{ARL} = \mathbf{q}^T(\mathbf{I} - \mathbf{Q})^{-1}\mathbf{1} \tag{9}$$

and

$$\mathrm{SDRL} = \sqrt{2\mathbf{q}^T(\mathbf{I} - \mathbf{Q})^{-2}\mathbf{Q1} - \mathrm{ARL}^2 + \mathrm{ARL}}, \tag{10}$$

respectively. In Equations (9) and (10), the matrix $\mathbf{I}$ is a $(v \times v)$ identity matrix and the initial probability vector $\mathbf{q} = (1, 0, ..., 0)^T$ has a unity in its first element and zeros elsewhere.

3 Results and discussions

In this section, the properties of the gamma distribution from a statistical perspective will be presented first. It is followed by a discussion of the obtained results. The probability density function of the gamma distribution is

$$f(x) = \frac{1}{\Gamma(a)b^a} x^{a-1} e^{-\frac{x}{b}}, \quad x > 0, \ a, b > 0, \tag{11}$$

where a and b correspond to the shape and scale parameters, respectively, while the $\Gamma(\cdot)$ in Equation (11) is defined as the gamma function. We denote this distribution as Gamma (a, b). The gamma distribution has a mean ab and a variance ab^2. As a decreases, the gamma distribution is more skewed to the right. Throughout this paper, we choose $b = 1$ in combination with $a \in \{1, 2, 4\}$ for ease of comparison. Note that the Gamma(1, 1) distribution is the most skewed among the three gamma distributions. It is then followed by the Gamma(2, 1) distribution and the Gamma(4, 1) distribution has the lowest degree of skewness.

In this paper, we outline the design of the k regions RS $\bar{X}$ chart under the normal distribution. We consider $k \in \{4, 7\}$ in the remaining of this paper. The optimal charts' parameters $(\{S_1, S_2, S_3, S_4\}, K)$ and $(\{S_1, S_2, S_3, S_4, S_5, S_6, S_7\}, K)$ for the 4 and 7 regions RS $\bar{X}$ charts, respectively, under the normal distribution, are computed via the developed optimization programmes in MATLAB software. These charts' parameters are computed when $n \in \{5, 10\}$ and $\delta_{\text{opt}} = 0.5$, together with their corresponding ARL and SDRL values computed using Equations (9) and (10), respectively. Here, δ_{opt} refers to the optimal process mean shift, in order to achieve a quick detection speed. It must be noticed that the optimal charting parameters must satisfy the in-control ARL $= 500$ when $n = \{5, 10\}$ for both the 4 and 7 regions RS $\bar{X}$ charts. The (ARL_0, SDRL_0) and (ARL_1, SDRL_1) are used to denote the in-control and out-of-control (ARL, SDRL) values, respectively.

Table 1 displays the (ARL_0, SDRL_0) performances for both the 4 and 7 regions RS $\bar{X}$ charts, respectively, under both normal and gamma distributions; while Tables 2 and 3 show the (ARL_1, SDRL_1) performances of the RS $\bar{X}$ charts for positive and negative mean shifts, respectively. The (ARL_0, SDRL_0) and (ARL_1, SDRL_1) values for the various gamma distributions shown in Tables 1 – 3 are determined through Monte Carlo simulations comprising $100{,}000$ replications. These values are computed when the charts' parameters are specifically designed for the normal distribution. For example, from Table 1, the (ARL_0, SDRL_0) values for the 4 regions RS $\bar{X}$ chart under Gamma(4, 1) distribution, are obtained as $(358.09, 355.43)$ when $n = 5$ using the optimal chart's parameters $(\{S_1, S_2, S_3, S_4\}, K) = (\{0, 1, 2, 4\}, 1.2432)$. Note that these optimal charting parameters are obtained under the normal distribution. Using the same charting parameters with $\delta = 0.25$, the 4 regions RS $\bar{X}$ chart's (ARL_1, SDRL_1) values are $(48.36, 45.04)$ for the Gamma(4, 1) distribution (see Table 2). Similarly, for a negative shift of $\delta = -0.25$, the (ARL_1, SDRL_1) values are $(50.77, 46.14)$ under Gamma(2, 1) distribution (refer to Table 3).

Table 1. (ARL_0, SDRL_0) values for the 4 and 7 regions RS $\bar{X}$ chart under normal and various gamma distributions with sample size, $n \in \{5, 10\}$.

	RS $\bar{X}$ Chart ($k = 4$)		RS $\bar{X}$ Chart ($k = 7$)	
	$\{S_1, S_2, S_3, S_4\}$ K $\{0, 1, 2, 4\}$ 1.2432	$\{S_1, S_2, S_3, S_4\}$ K $\{0, 2, 4, 7\}$ 1.2432	$\{S_1, S_2, S_3, S_4, S_5, S_6, S_7\}$ K $\{0, 1, 2, 4, 5, 7, 10\}$ 1.3554	$\{S_1, S_2, S_3, S_4, S_5, S_6, S_7\}$ K $\{0, 0, 1, 2, 3, 4, 6\}$ 1.1952
n	5	10	5	10
Distributions	(ARL_0, SDRL_0)	(ARL_0, SDRL_0)	(ARL_0, SDRL_0)	(ARL_0, SDRL_0)
Normal	(500.00, 496.25)	(500.00, 496.25)	(500.00, 495.48)	(500.00, 496.88)
Gamma(4, 1)	(358.09, 355.43)	(414.04, 410.94)	(404.89, 401.32)	(384.74, 382.33)
Gamma(2, 1)	(286.84, 284.70)	(358.09, 355.43)	(343.01, 340.06)	(319.29, 317.26)
Gamma(1, 1)	(214.10, 212.51)	(286.84, 284.70)	(265.44, 263.20)	(245.80, 244.19)

Table 2. (ARL_1, SDRL_1) values for the 4 and 7 regions RS $\bar{X}$ charts under normal and various gamma distributions when $n \in \{5, 10\}$ and $\delta \in \{0.25, 0.50, 0.75, 1.00, 1.50, 2.00\}$.

		RS $\bar{X}$ Chart ($k = 4$)		RS $\bar{X}$ Chart ($k = 7$)	
		$\{S_1, S_2, S_3, S_4\}$	$\{S_1, S_2, S_3, S_4\}$	$\{S_1, S_2, S_3, S_4, S_5, S_6, S_7\}$	$\{S_1, S_2, S_3, S_4, S_5, S_6, S_7\}$
		K	K	K	K
		$\{0, 1, 2, 4\}$	$\{0, 2, 4, 7\}$	$\{0, 1, 2, 4, 5, 7, 10\}$	$\{0, 0, 1, 2, 3, 4, 6\}$
		1.2432	1.2432	1.3554	1.1952
n		5	10	5	10
Distributions	δ	(ARL_1, SDRL_1)	(ARL_1, SDRL_1)	(ARL_1, SDRL_1)	(ARL_1, SDRL_1)
Normal	0.25	(51.00, 47.01)	(23.01, 19.26)	(45.89, 41.55)	(23.33, 19.79)
	0.50	(10.65, 7.34)	(5.57, 2.86)	(10.18, 6.70)	(5.34, 2.88)
	0.75	(5.06, 2.46)	(3.06, 1.19)	(5.04, 2.29)	(2.81, 1.18)
	1.00	(3.31, 1.32)	(2.05, 0.83)	(3.39, 1.21)	(1.87, 0.75)
	1.50	(1.88, 0.78)	(1.16, 0.38)	(2.02, 0.73)	(1.12, 0.33)
	2.00	(1.24, 0.45)	(1.00, 0.07)	(1.35, 0.50)	(1.00, 0.06)
Gamma(4, 1)	0.25	(48.36, 45.04)	(23.19, 19.69)	(45.05, 41.30)	(22.86, 19.64)
	0.50	(10.79, 7.58)	(5.57, 2.85)	(10.23, 6.80)	(5.37, 2.90)
	0.75	(5.05, 2.42)	(3.06, 1.18)	(5.01, 2.20)	(2.83, 1.18)
	1.00	(3.31, 1.29)	(2.06, 0.82)	(3.39, 1.18)	(1.88, 0.74)
	1.50	(1.91, 0.76)	(1.16, 0.37)	(2.04, 0.72)	(1.12, 0.32)
	2.00	(1.24, 0.44)	(1.00, 0.04)	(1.37, 0.50)	(1.00, 0.03)
Gamma(2, 1)	0.25	(47.09, 44.05)	(23.23, 19.84)	(44.64, 41.12)	(22.68, 19.59)
	0.50	(10.82, 7.63)	(5.57, 2.83)	(10.21, 6.80)	(5.38, 2.90)
	0.75	(5.04, 2.38)	(3.06, 1.17)	(4.98, 2.13)	(2.84, 1.18)
	1.00	(3.32, 1.28)	(2.08, 0.82)	(3.39, 1.17)	(1.89, 0.74)
	1.50	(1.92, 0.75)	(1.15, 0.36)	(2.05, 0.71)	(1.12, 0.32)
	2.00	(1.24, 0.43)	(1.00, 0.02)	(1.38, 0.49)	(1.00, 0.01)
Gamma(1, 1)	0.25	(45.36, 42.68)	(23.27, 20.03)	(44.06, 40.88)	(22.46, 19.54)
	0.50	(10.82, 7.62)	(5.56, 2.79)	(10.14, 6.70)	(5.40, 2.88)
	0.75	(5.03, 2.31)	(3.07, 1.16)	(4.93, 2.00)	(2.85, 1.18)
	1.00	(3.32, 1.27)	(2.08, 0.81)	(3.40, 1.17)	(1.90, 0.73)
	1.50	(1.93, 0.75)	(1.15, 0.36)	(2.06, 0.70)	(1.11, 0.31)
	2.00	(1.24, 0.43)	(1.00, 0.00)	(1.39, 0.49)	(1.00, 0.00)

When the process data comes from a gamma distribution, it is anticipated that the optimal RS $\bar{X}$ chart's parameters under the normal distribution will result in different control chart's performances, depending on the choice of the shape parameter a. Based on Table 1, i.e., the in-control cases, when a decreases (more skewed to the right) and $n = 5$, the (ARL_0, SDRL_0) values are far away from the normal distribution, indicating a higher occurrence of false alarms. It must be noted that the false alarm rate has an inverse relationship with the ARL_0. The 7 regions RS $\bar{X}$ chart has lower false alarm rates compared to the 4 regions RS $\bar{X}$ chart for all specified gamma distributions when $n = 5$. To illustrate, under the Gamma(2, 1) distribution with $n = 5$, the (ARL_0, SDRL_0) values for the 4 and 7 regions RS $\bar{X}$ chart are (286.84, 284.70) and (358.09, 355.43), respectively. Additionally, as shown in Table 1,

Table 3. (ARL_1, SDRL_1) values for the 4 and 7 regions RS $\bar{X}$ charts under normal and various gamma distributions when $n \in \{5, 10\}$ and $\delta \in \{-0.25, -0.50, -0.75, -1.00, -1.50, -2.00\}$.

		RS $\bar{X}$ Chart ($k = 4$)		RS $\bar{X}$ Chart ($k = 7$)	
		$\{S_1, S_2, S_3, S_4\}$ K $\{0, 1, 2, 4\}$ 1.2432	$\{S_1, S_2, S_3, S_4\}$ K $\{0, 2, 4, 7\}$ 1.2432	$\{S_1, S_2, S_3, S_4, S_5, S_6, S_7\}$ K $\{0, 1, 2, 4, 5, 7, 10\}$ 1.3554	$\{S_1, S_2, S_3, S_4, S_5, S_6, S_7\}$ K $\{0, 0, 1, 2, 3, 4, 6\}$ 1.1952
n		5	10	5	10
Distributions	δ	(ARL_1, SDRL_1)	(ARL_1, SDRL_1)	(ARL_1, SDRL_1)	(ARL_1, SDRL_1)
Normal	−0.25	(51.00, 47.01)	(23.01, 19.26)	(45.89, 41.55)	(23.33, 19.79)
	−0.50	(10.65, 7.34)	(5.57, 2.86)	(10.18, 6.70)	(5.34, 2.88)
	−0.75	(5.06, 2.46)	(3.06, 1.19)	(5.04, 2.29)	(2.81, 1.18)
	−1.00	(3.31, 1.32)	(2.05, 0.83)	(3.39, 1.21)	(1.87, 0.75)
	−1.50	(1.88, 0.78)	(1.16, 0.38)	(2.02, 0.73)	(1.12, 0.33)
	−2.00	(1.24, 0.45)	(1.00, 0.07)	(1.35, 0.50)	(1.00, 0.06)
Gamma(4, 1)	−0.25	(51.40, 46.91)	(22.64, 18.68)	(46.22, 41.36)	(23.76, 19.89)
	−0.50	(10.43, 7.02)	(5.56, 2.83)	(10.04, 6.49)	(5.30, 2.83)
	−0.75	(5.05, 2.43)	(3.05, 1.20)	(5.04, 2.30)	(2.79, 1.18)
	−1.00	(3.32, 1.32)	(2.02, 0.84)	(3.40, 1.22)	(1.85, 0.76)
	−1.50	(1.84, 0.79)	(1.16, 0.38)	(2.00, 0.74)	(1.13, 0.34)
	−2.00	(1.23, 0.45)	(1.01, 0.10)	(1.34, 0.51)	(1.01, 0.08)
Gamma(2, 1)	−0.25	(50.77, 46.14)	(22.43, 18.39)	(46.30, 41.24)	(23.88, 19.88)
	−0.50	(10.32, 6.87)	(5.55, 2.81)	(9.97, 6.40)	(5.29, 2.80)
	−0.75	(5.04, 2.41)	(3.05, 1.20)	(5.03, 2.30)	(2.78, 1.17)
	−1.00	(3.32, 1.31)	(2.01, 0.85)	(3.41, 1.22)	(1.84, 0.76)
	−1.50	(1.82, 0.79)	(1.16, 0.38)	(2.00, 0.74)	(1.13, 0.34)
	−2.00	(1.23, 0.45)	(1.01, 0.11)	(1.33, 0.51)	(1.01, 0.09)
Gamma(1, 1)	−0.25	(48.40, 43.66)	(22.10, 17.96)	(46.62, 41.27)	(23.98, 19.82)
	−0.50	(10.20, 6.69)	(5.53, 2.79)	(9.84, 6.24)	(5.26, 2.76)
	−0.75	(5.00, 2.38)	(3.06, 1.20)	(5.00, 2.27)	(2.77, 1.16)
	−1.00	(3.33, 1.30)	(2.00, 0.85)	(3.41, 1.21)	(1.82, 0.77)
	−1.50	(1.80, 0.79)	(1.16, 0.38)	(1.98, 0.75)	(1.13, 0.34)
	−2.00	(1.22, 0.46)	(1.01, 0.12)	(1.31, 0.51)	(1.01, 0.10)

when n increases from 5 to 10, we observe an increase in the (ARL_0, SDRL_0) values for the 4 regions RS $\bar{X}$ chart across all the gamma distributions. This means that adding more sample size will improve the statistical efficiency of the 4 regions RS $\bar{X}$ chart. However, as n increases, there is a contrasting deterioration in the (ARL_0, SDRL_0) values for the 7 regions RS $\bar{X}$ chart. This unexpected result may pose challenges for practitioners in accurately accessing the control performance under the gamma process.

By referring to Tables 2 and 3, i.e., the out-of-control cases, it should be noted that the (ARL_1, SDRL_1) values of the RS $\bar{X}$ charts for positive and negative mean shifts under the normal distribution are identical. This symmetry arises due to the characteristics of the normal distribution. As a decreases, the (ARL_1, SDRL_1) values for the RS $\bar{X}$ charts under the gamma distributions start deviating from the normal distribution (see Tables 2 and 3). This

is because of the increase in the skewness of gamma distribution. For instance, when $\delta = 0.25$ and $n = 5$, the $(\mathrm{ARL}_1, \mathrm{SDRL}_1)$ values for the 4 regions RS $\bar{X}$ chart are (51.00, 47.01), (48.36, 45.04), (47.09, 44.05) and (45.36, 42.68) under normal, Gamma(4, 1), Gamma(2, 1) and Gamma(1, 1) distributions, respectively. Moreover, based on Table 2, when $n = 5$ and $0.25 \leq \delta \leq 0.75$, the 7 regions RS $\bar{X}$ chart surpasses the 4 regions RS $\bar{X}$ chart for all the gamma distributions. For $\delta \geq 1.00$, it is showed that both the 4 and 7 regions RS $\bar{X}$ charts have quite similar statistical performances in the detection of moderate and large process mean shifts under gamma distributions. For example, under the Gamma(1, 1) distribution with $\delta = 1.00$ and $n = 5$, the ARL_1 values for the 4 and 7 regions RS $\bar{X}$ chart are 3.32 and 3.40, respectively, which are close to each other. Furthermore, for negative mean shifts (refer to Table 3), similar performance trends are observed. Specifically, when $n = 5$ and $-0.75 \leq \delta \leq -0.25$, the 7 regions RS $\bar{X}$ chart consistently demonstrates superior ARL_1 performances compared to the 4 regions RS $\bar{X}$ chart for all the gamma distributions. When $\delta \leq -1.00$, both the 4 and 7 regions RS $\bar{X}$ charts have comparable performances under gamma distributions. Besides, for $n = 10$, it is evident that the detection speed for both the 4 and 7 regions RS $\bar{X}$ charts has improved for all the gamma distributions in both cases of positive and negative mean shifts (see Tables 2 and 3). Note that a smaller ARL_1 value corresponds to a faster chart detection speed. From Table 2, when $n = 10$, the 7 regions RS $\bar{X}$ chart consistently outperforms the 4 regions RS $\bar{X}$ chart for all positive mean shift sizes, demonstrating superior detection speed across all the gamma distributions. For the cases with negative mean shifts, the 7 regions RS $\bar{X}$ chart exhibits overall better out-of-control performances compared to the 4 regions RS $\bar{X}$ chart under gamma distributions (refer to Table 3).

4 Conclusions

Throughout this paper, we thoroughly examine the (ARL, SDRL) performances of the RS $\bar{X}$ chart designed under the normal distribution when the underlying process adheres to a gamma distribution. For the in-control cases, it is clear that the ARL_0 values decrease as the shape parameter a decreases for the RS $\bar{X}$ charts. Excessive false alarms are undesirable as practitioners may lose their confidence in using the control charts and increase the inspection costs for unnecessary adjustments. When $n = 5$, the 7 regions RS $\bar{X}$ chart performs better in the detection of small positive and negative process mean shifts ($0.25 \leq \delta \leq 0.75$ and $-0.75 \leq \delta \leq -0.25$); while the 4 and 7 regions RS $\bar{X}$ charts exhibit comparable detection speeds in identifying moderate and large process mean shifts ($\delta \geq 1.00$ and $\delta \leq -1.00$). Besides, increasing the sample size n will lead to an improvement in the detection speed of the RS $\bar{X}$ chart under both distributions. The inconsistency in the performances of the RS $\bar{X}$ chart across gamma distributions may be due to the use of wrong charting parameters, which were originally designed for the normal distribution. Therefore, in future research, the development of new theoretical formulae, and optimal charting parameters specifically tailored for the gamma process can be conducted for the RS $\bar{X}$ chart.

This research paper is supported by the Ministry of Higher Education (MOHE) Malaysia and Heriot-Watt University Malaysia under Fundamental Research Grant Scheme (FGRS), no. FRGS/1/2021/HWUM/02/01.

References

1. W.A. Shewhart, Economic control of quality of manufactured product, New York: Van Nostrand (1931)

2. S.W. Roberts, Technometrics, **8**(3), 411 – 430 (1966)
3. J.H. Reynolds, J. Qual. Technol., **3**(1), 23 – 27 (1971)
4. A.H. Jaehn, Qual., **26**(10), 51 – 53 (1987)
5. R.B. Davis, C. Jin, Y. Guo, Commun. Stat. – Theory Methods., **23**(12), 3557 – 3565 (1994)
6. C.W. Champ, S.E. Rigdon, J. Qual. Technol., **29**(4), 407 – 417 (1997)
7. S. Parkhideh, B. Parkhideh, Int. J. Prod. Res., **36**(8), 2259 – 2267 (1998)
8. V. Aguirre-Torres, D. Reyes-López, Qual. Eng., **12**(1), 7 – 12 (1999)
9. R.B. Davis, T.C. Krehbiel, Commun. Stat. Simul. Comput., **31**(1), 91 – 96 (2002)
10. C. Acosta-Mejia, J.J.J. Pignatiello, Commun. Stat. Simul. Comput., **39**(5), 921 – 932 (2010)
11. C.K. Sitt, M.B.C. Khoo, M. Shamsuzzaman, C.H. Chen, Int. J. Adv. Manuf. Technol., **70**(5), 1487 – 1504 (2014)
12. C.A. Acosta-Mejia, L. Rincon, Commun. Stat. – Theory Methods., **43**(20), 4371 – 4383 (2014)
13. S. Saha, M.B.C. Khoo, W.L. Teoh, M.H. Lee, Qual. Reliab. Eng. Int., **33**(8), 1885 – 1899 (2017)
14. W.L. Teoh, M.B.C. Khoo, P. Castagliola, W.C. Yeong, S.Y. The, Eur. J. Oper. Res., **257**(1), 144 – 158 (2017)
15. A.J.X. Lim, M.B.C. Khoo, W.L. Teoh, A, Haq, Comput. Ind. Eng., **109**, 84 – 95 (2017)
16. W.C. Yeong, S.L. Lim, M.B.C. Khoo, P.S. Ng, Z.L. Chong, J. Stat. Comput. Simul., **92**(15), 3150 – 3166 (2022)
17. W.C. Yeong, Y.Y. Tan, S.L. Lim, K.W. Khaw, M.B.C. Khoo, Qual. Technol. Quant. Manag., **21**(2), 177 – 199 (2024)
18. D.C. Montgomery, *Introduction to statistical quality control*, 8th ed. New York: John Wiley & Sons (2019)
19. W.L. Teoh, W.C. Yeong, M.B.C. Khoo, S.Y. Teh. Acad. J. Sci., **5**(1), 237 – 252 (2016)
20. D. Karagöz, C. Hamurkaroğlu, Adv. Methodol. Stat., **9**, 95 – 106 (2012)
21. A. Saghir, L. Ahmad, M. Aslam, Commun. Stat. Simul. Comput., **50**(10), 3046 – 3059 (2021)
22. Y.S. Chang, D.S. Bai, Qual. Reliab. Eng. Int., **17**(5), 397 – 406 (2001)